

Undetected Error Probability in the Short Blocklength Regime: Approaching Finite-Blocklength Bounds with Polar Codes

Alexander Sauter, *Graduate Student Member, IEEE*, A. Oguz Kislal, Giuseppe Durisi, *Senior Member, IEEE*, Gianluigi Liva, *Senior Member, IEEE*, Balázs Matuz, *Senior Member, IEEE*, and Erik G. Ström, *Fellow, IEEE*

Abstract—We analyze the trade-off between the undetected error probability (i.e., the probability that the channel decoder outputs an erroneous message without detecting the error) and the total error probability in the short blocklength regime. We address the problem by developing two new finite blocklength achievability bounds, which we use to benchmark the performance of two coding schemes based on polar codes with outer cyclic redundancy check (CRC) codes—also referred to as CRC-aided (CA) polar codes. The first bound is obtained by considering an outer detection code, whereas the second bound relies on a threshold test applied to the generalized information density. Similarly, in the first CA polar code scheme, we reserve a fraction of the outer CRC parity bits for error detection, whereas in the second scheme, we apply a threshold test (specifically, Forney’s optimal rule) to the output of the successive cancellation list decoder. Numerical simulations performed on the binary-input AWGN channel reveal that, in the short-blocklength regime, the threshold-based approach is superior to the CRC-based approach, both in terms of bounds and performance of CA polar code schemes. We also consider the case of decoding with noisy channel-state information, which leads to a mismatched decoding setting. Our results illustrate that, differently from the previous case, in this scenario, the CRC-based approach outperforms the threshold-based approach, which is more sensitive to the mismatch.

Index Terms—Ultra-reliable low-latency communications, polar codes, finite-length bounds, error detection.

I. INTRODUCTION

THE design of efficient short error correcting codes is subject of renewed interest due to emerging applications envisaged in 5G and beyond [2], [3]. Consider as an example

This paper was presented in part at the 57th Annual Conference on Information Sciences and Systems (CISS) [1].

Alexander Sauter is with the Institute for Communications Engineering, School of Computation, Information, and Technology, Technical University of Munich, Arcisstrasse 21, D-80333 Munich, Germany, and with the German Aerospace Center, Münchener Strasse 20, D-82234 Wessling, Germany. Gianluigi Liva is with the German Aerospace Center, Münchener Strasse 20, D-82234 Wessling, Germany (e-mail: {alexander.sauter, gianluigi.liva,}@dlr.de). A. Oguz Kislal, Giuseppe Durisi, and Erik G. Ström are with the Department of Electrical Engineering, Chalmers University of Technology, Gothenburg 41296, Sweden (e-mail: {kislal, durisi, erik.strom}@chalmers.se). Balázs Matuz is with the Huawei Munich Research Center, 80992 Munich, Germany (e-mail: balazs.matuz@huawei.com).

Alexander Sauter and Gianluigi Liva acknowledge the financial support by the Federal Ministry of Education and Research of Germany in the program of “Souverän. Digital. Vernetzt.”, by the joint project 6G-RIC, project identification number: 16KISK022, and by the DLR-funded project “DIAL”.

This paper was supported in part by the Swedish Research Council under grants 2021-04970 and 2022-04471.

the 3GPP 5G NR standard. In the case of enhanced mobile broadband (eMBB) links, small data units play an essential role in the control channel. In the massive machine-type communication (mMTC) setting, a large number of devices transmit short packets in a sporadic and uncoordinated manner. In ultra-reliable low-latency communications (URLLC), delay constraints require the use of short error correcting codes. Furthermore, strict reliability requirements call for low post-decoding error rates. The URLLC scenario is especially relevant in the context of intelligent mobility, industry automation, cyber-physical systems, and wireless telecommand systems (see, e.g., [4], [5, Chapter 4]).

The reliability requirements of URLLC systems are typically expressed in terms of block error probability at the decoder output. However, this is not sufficient in certain mission-critical applications, for which it is essential to distinguish between two types of decoding errors: *detected* and *undetected* errors. An error is detected if the channel decoder signals to the upper layers a decoding failure (*erasure*). An error is undetected if the decoder outputs an erroneous message, which is forwarded to the upper layers. In the absence of additional error detection capabilities in the upper layers—provided by, e.g., additional cyclic redundancy check (CRC) codes—undetected errors can be particularly harmful [6]. It is, hence, imperative to assess the performance of an error correction algorithm in terms of *both* the total error probability (TEP) and the undetected error probability (UEP).

The design of channel codes capable of providing low UEP is challenging at short blocklengths. When the blocklength is large, error detection capabilities can be provided by appending to the data packet a sufficiently long CRC code, which is used for error detection after decoding. The key observation is that, for long packets, the addition of the CRC code parity bits causes only a negligible rate loss, and, hence, a small TEP penalty. On the contrary, for short packets, the use of a CRC code as error detection mechanism¹ can result in an unacceptable rate loss and, hence, a significant TEP penalty. A

¹CRC codes are sometimes used, in concatenation with short polar codes, to improve the error correction performance of the inner polar code under successive cancellation list decoding [7]. This setting should not be confused with the one where the outer CRC is used purely for error detection.

more appealing solution is the use of an *incomplete*² decoder, capable of detecting decoding errors with a sufficiently high probability.

An optimum incomplete decoding rule was introduced and analyzed using information-theoretic tools by Forney in [9]. The approach of [9] can be interpreted as the application of (complete) maximum likelihood (ML) decoding, followed by a post-decoding threshold test. The test is used to either accept or discard the ML decoder decision. More specifically, Forney demonstrated that the decoder that optimally trades between TEP and UEP operates as follows: it outputs the message whose likelihood is at least 2^{nT} times larger than the sum of the likelihood of all other messages. If no message satisfies this condition, it declares an erasure. Here, n denotes the blocklength, and T is a suitably chosen threshold. Forney also performed an error-exponent analysis of this decoding rule, demonstrating that both TEP and UEP decay exponentially fast with the blocklength for discrete memoryless channel (DMC). Forney’s decoding metric can be efficiently evaluated for certain code classes (e.g., for terminated convolutional codes [10], [11]), or it can be well approximated for other code classes (e.g., for codes based on compact tail-biting trellises [12], [13]). Suboptimal tests are proposed and analyzed in [14], [15]. Heuristic threshold tests are introduced in [16] for CA polar codes [17], [18] under successive cancellation list (SCL) decoding [19]. Error detection for polar codes under SCL via typicality check or by using a random linear code as outer error detection code was analyzed in [20].

Forney’s error-exponent analysis has been extended in various directions in the literature. In [21], the author provides error exponent bounds that are at least as tight as Forney’s error exponent bounds and are simpler to evaluate in certain cases. This analysis was further extended in [22], where the exact random coding exponent is determined for the i.i.d. codebook ensemble under certain channel-symmetry conditions. In [23], the author derives TEP and UEP bounds for spherical codes over the additive white Gaussian noise (AWGN) channel under a suboptimal decoding rule. The authors of [24] provide bounds for structured codes. Specifically, using the distance distribution of a linear block code ensemble, they improve Forney’s bounds for some linear block code ensembles. In [25]–[27], Forney’s result is generalized for the case in which constant composition codes are used. All these results, however, rely on Gallager’s error exponent framework, which typically yields loose bounds for short blocklengths and error probabilities of interest for URLLC applications [28], [29].

In [30], erasure decoding is analyzed in the moderate deviation regime, i.e., the regime in which the code rate tends to capacity at a rate slower than $n^{-1/2}$ and the error probability

decays with n .³ Notably, this analysis employs a suboptimal decoder that involves thresholding the information density rather than Forney’s optimal metric, which is not analytically tractable in this regime. In [31], the second-order term in the asymptotic expansion of the maximum coding rate, for a given fixed error probability, in the asymptotic limit of large blocklength is evaluated for erasure decoding. Similar to [30], the achievability part of the proof relies on a suboptimal threshold decoder. The analyses in [30] and [31] do not aim to obtain numerically computable bounds for short blocklengths. Hence, they do not directly provide ways to benchmark the performance of actual coding schemes in the short-packet regime. As we shall see, employing a suboptimal decoder that involves thresholding the (generalized) information density will prove to be an effective approach to obtain numerically computable bounds.

Contributions: In this work, we study the TEP and the UEP for short polar codes, concatenated with outer CRC codes, which we shall refer to as CRC-aided (CA) polar codes, in the following. We focus on this code class because of its excellent performance in the short block length regime with low-complexity SCL decoding [32]. We introduce two error detection methods. A first method relies on “splitting” the parity bits of the CRC code: a portion of the bits is used to prune the SCL decoder list, whereas the remaining parity bits are used for error detection. The second approach is based on the optimal threshold test of [9], adapted to SCL decoding. The TEP and UEP performance under the two approaches are analyzed over the binary-input additive white Gaussian noise (biAWGN) channel, and over the block-memoryless phase-noise channel [33] with imperfect channel state information (CSI) at the receiver. To benchmark the performance of these short polar codes, we devise two novel information-theoretic achievability bounds. Specifically, in agreement with the first detection method, the first bound is obtained by using an outer decoder for error detection. Furthermore, in agreement with the second detection method, the second bound relies on a threshold decoder (although, following [30], [31], a suboptimal decoder is used for analytical tractability). Unlike Forney’s bound, both bounds are based on the random coding union (RCU) bound [28, Thm. 16]. The RCU bound requires the evaluation of a certain tail probability, which is not known in closed form and must be evaluated numerically. This is extremely time-consuming due to the low error probabilities of interest in URLLC. To tackle this issue, we present a saddlepoint approximation, which generalizes the one reported in [34]. Numerical experiments lead to the following observations:

- The two novel achievability bounds outperform Forney’s bound for the biAWGN channel in the short blocklength regime and for the TEP and UEP considered in the paper. Furthermore, the bound obtained through the suboptimal threshold decoder outperforms the one based on an outer

²A complete decoder is a decoder returning always a valid codeword. In contrast, an incomplete decoder returns a valid codeword or an erasure, i.e., a decoding failure flag. Any blockwise maximum likelihood decoder or the successive cancellation decoder of polar codes are examples of complete decoders. Decoders based on the belief propagation algorithm and bounded-distance decoders are incomplete decoders. See, e.g., [8, Ch. 1].

³As a comparison, in the error-exponent regime, the rate is fixed and the error probability decays exponentially with n . Another regime of interest is the second-order asymptotic regime, where the rate converges to capacity at a rate of $n^{-1/2}$ and the error probability is fixed.

code. However, the gap between the two bounds becomes less pronounced as the blocklength increases. The simulation results for CA polar codes over the biAWGN channel confirm these insights: the threshold test that approximates the decision metric of [9] by using the SCL decoder output outperforms the detection method based on an outer CRC for short blocklengths. Also in this case, the gain vanishes as the blocklength grows.

- Over the block-memoryless phase-noise channel with imperfect CSI, the gap between the two achievability bounds is drastically reduced. Simulation results for CA polar codes follow the trend displayed by the bounds. This suggests that, in the presence of inaccurate CSI, error detection by means of an outer CRC code is more robust and, hence, preferable. On the contrary, threshold-based techniques that rely on a mismatched likelihood suffer from a significant performance loss for a wide range of blocklengths.

The remainder of the manuscript is organized as follows. In Section II, we introduce the notation and the system model. In Section III, we review Forney's optimum erasure decoder, as well as its error exponent analysis [9]. Then, two new achievability bounds are presented, and their numerical evaluation is discussed. Error detection strategies for CA polar codes are described in Section IV. Numerical results are provided in Section V and conclusions follow in Section VI.

II. PRELIMINARIES

A. Notation

We denote vectors by small bold letters, e.g., \mathbf{x} , and sets by capital calligraphic letters, e.g., \mathcal{X} . The cardinality of a set \mathcal{X} is denoted by $|\mathcal{X}|$. We use \mathbb{F}_2 for the binary finite field with elements $\{0, 1\}$ and \mathbb{N}_0 to denote the set of natural numbers including 0. We write $\log(\cdot)$ to denote the natural logarithm and $\log_2(\cdot)$ to denote the base-2 logarithm. Moreover, $\|\cdot\|$ stands for the ℓ_2 -norm, $\mathbb{P}[\cdot]$ for the probability of an event, $\mathbb{E}[\cdot]$ for the expectation operator, $Q(\cdot)$ for the Gaussian Q -function, and $\mathbb{1}(\cdot)$ for the indicator function. Finally, for two functions $f(n)$ and $g(n)$, the notation $f(n) = o(g(n))$ means that $\lim_{n \rightarrow \infty} f(n)/g(n) = 0$.

B. System Model

We consider an arbitrary discrete-time communication channel that maps input symbols from the set \mathcal{X} into output symbols from the set \mathcal{Y} . Specifically, let $\mathbf{x} = [x_1, \dots, x_n] \in \mathcal{X}^n$ and $\mathbf{y} = [y_1, \dots, y_n] \in \mathcal{Y}^n$ be vectors containing n channel inputs and their corresponding outputs. The channel is defined by its transition probability⁴ $P_{\mathbf{y}|\mathbf{x}}(\mathbf{y}|\mathbf{x})$.

We next define the notion of a channel code. Similar to, e.g., [35], it will turn out convenient to focus on the class of *randomized* coding schemes, i.e., coding schemes in which

a common source of randomness (which we denote by u) is available at both transmitter and receiver. This randomness is used to initialize the encoder and decoder.

Definition 1. An $(n, k, \epsilon_T, \epsilon_U)$ -code for the channel $P_{\mathbf{y}|\mathbf{x}}$ consists of

- A discrete random variable u with distribution P_u defined on a set \mathcal{U} with $|\mathcal{U}| \leq 2$ that is revealed to both the transmitter and the receiver before the start of transmission. This allows the transmitter and the receiver to time-share between up to two deterministic codes.
- An encoder $\phi : \mathcal{U} \times \{1, \dots, 2^k\} \rightarrow \mathcal{X}^n$ that maps a message w , which we assume to be uniformly distributed on $\{1, \dots, 2^k\}$, to a codeword in the set $\mathcal{C}_u \subset \mathcal{X}^n$.
- An erasure decoder $g : \mathcal{U} \times \mathcal{Y}^n \rightarrow \{0, 1, \dots, 2^k\}$ that maps the received vector to one of the messages in $\{1, \dots, 2^k\}$, or declares an erasure, which we indicate by the extra symbol 0. Let, for a given u , $\mathcal{D}_{u, \hat{w}} = g^{-1}(u, \hat{w}) \subset \mathcal{Y}^n$ denote the decoding region associated to each decoder output $\hat{w} \in \{0, 1, \dots, 2^k\}$ and assume that these decoding regions form a partition of \mathcal{Y}^n for each fixed u . We require that the TEP and UEP do not exceed ϵ_T and ϵ_U , respectively. Mathematically,

$$\frac{1}{2^k} \sum_{m=1}^{2^k} \sum_{\substack{m'=0 \\ m' \neq m}}^{2^k} \mathbb{P}[\mathbf{y} \in \mathcal{D}_{u, m'} | w = m] \leq \epsilon_T \quad (1)$$

$$\frac{1}{2^k} \sum_{m=1}^{2^k} \sum_{\substack{m'=1 \\ m' \neq m}}^{2^k} \mathbb{P}[\mathbf{y} \in \mathcal{D}_{u, m'} | w = m] \leq \epsilon_U \quad (2)$$

where in (1) and (2) the probabilities are computed over the pair (u, \mathbf{y}) .

III. NON-ASYMPTOTIC ACHIEVABILITY BOUNDS ON TEP AND UEP

In this section, we will first review Forney's optimal erasure decoder. Then, we will introduce two novel finite-blocklength bounds, which are tailored to the short-blocklength regime. These two bounds rely on error detection strategies similar to the ones we will consider for CA polar codes in Section IV.

A. Optimum Erasure Decoder

Forney, in his seminal paper [9], showed that the optimal erasure decoder,⁵ has the following structure: the decoder outputs the message corresponding to the codeword \mathbf{x} that satisfies

$$\Lambda(\mathbf{x}, \mathbf{y}) > 2^{nT} \quad (3)$$

where $T \geq 0$ is a parameter⁶ that controls the tradeoff between ϵ_U and ϵ_T , and

$$\Lambda(\mathbf{x}, \mathbf{y}) = \frac{P_{\mathbf{y}|\mathbf{x}}(\mathbf{y}|\mathbf{x})}{\sum_{\mathbf{x}' \in \mathcal{C} \setminus \{\mathbf{x}\}} P_{\mathbf{y}|\mathbf{x}}(\mathbf{y}|\mathbf{x}')}. \quad (4)$$

⁵The decoder is optimal in the sense that no other decoder can achieve simultaneously a lower ϵ_T and a lower ϵ_U .

⁶When $T < 0$, the decoding regions are not disjoint and multiple codewords satisfy (3). In this case, the decoder puts out a list of messages corresponding to all codewords satisfying (3). In agreement with Definition 1, we will focus on the case $T \geq 0$.

⁴To keep the notation simple, we have chosen to specify the transition probability in terms of the conditional probability mass function $P_{\mathbf{y}|\mathbf{x}}(\mathbf{y}|\mathbf{x})$, which requires the set \mathcal{Y} to have finite cardinality. However, our analysis is general and can be applied also to channels with continuous input and output. In this case, $P_{\mathbf{y}|\mathbf{x}}(\mathbf{y}|\mathbf{x})$ should be replaced by the conditional probability density function $p_{\mathbf{y}|\mathbf{x}}(\mathbf{y}|\mathbf{x})$.

If no codeword in the codebook satisfies (3), the decoder declares an erasure. We note that the channel law $P_{\mathbf{y}|\mathbf{x}}(\mathbf{y}|\mathbf{x})$ needs to be known at the receiver to evaluate (4) and that the decoder puts out the ML decision when (3) is satisfied.

A characterization of the achievable $(\epsilon_\tau, \epsilon_u)$ pairs under this decoder over a DMC was provided in [9] through a random coding error exponent analysis (see, e.g., [21], [22] for more recent extensions). In particular, it was shown that for an arbitrary input distribution P_x , there exists a deterministic block code of length n and rate $R = k/n$ that simultaneously satisfies $\epsilon_\tau \leq \epsilon_\tau^F$ and $\epsilon_u \leq \epsilon_u^F$, where⁷

$$\epsilon_\tau^F = 2^{-nE_1(R, T, P_x)} \quad (5)$$

$$\epsilon_u^F = 2^{-nE_2(R, T, P_x)} \quad (6)$$

and where

$$E_1(R, T, P_x) = \max_{0 \leq s \leq \rho \leq 1} [E_0(s, \rho, P_x) - \rho R - sT] \quad (7)$$

$$E_2(R, T, P_x) = E_1(R, T, P_x) + T \quad (8)$$

with

$$E_0(s, \rho, P_x) = -\log_2 \sum_{y \in \mathcal{Y}} \left(\sum_{x \in \mathcal{X}} P_x(x) P_{y|x}(y|x)^{1-s} \right) \times \left(\sum_{x' \in \mathcal{X}} P_x(x') P_{y|x'}(y|x')^{s/\rho} \right)^\rho. \quad (9)$$

Through quantization of the channel inputs and outputs, one can evaluate these bounds for continuous channels as well. Note that when $T = 0$, we have that $E_1(R, T, P_x) = E_2(R, T, P_x)$ and these two terms coincide also with Gallager error exponent, derived under the assumption of ML decoding [9, p. 210].

As we shall see in Section V, the bounds (5)–(6) are not accurate in the short-blocklength regime, for the error probabilities typically considered in URLLC. Unfortunately, analyzing Forney's decoder using the probabilistic tools developed for the short-blocklength regime is challenging [30], [31]. To tackle this issue, it will turn out convenient to use suboptimal decoders. We next introduce two finite-blocklength achievability bounds that rely on such suboptimal decoders, as well as on the RCU bound [28, Thm. 16].

B. Achievability Bound via CRC Outer Code

We first consider an erasure decoder that relies on a CRC outer code for error detection. The finite-blocklength performance of such a scheme was analyzed in [36], where the authors approximate the TEP ϵ_τ using the so-called normal approximation [28, Eq. (1)], and the UEP by $\epsilon_u \approx \epsilon_\tau 2^{-\Delta}$, where Δ is the number of parity bits added by the CRC outer code. Next, we present a rigorous finite-blocklength achievability bound for this scheme.

Theorem 1. *For an arbitrary input distribution P_x and for every $\Delta \in \mathbb{N}_0$, there exists an $(n, k, \epsilon_\tau, \epsilon_u)$ -code for the*

channel $P_{\mathbf{y}|\mathbf{x}}(\mathbf{y}|\mathbf{x})$ simultaneously satisfying $\epsilon_\tau \leq \epsilon_\tau^{\text{ub},1}$ and $\epsilon_u \leq \epsilon_u^{\text{ub},1}$, where

$$\epsilon_\tau^{\text{ub},1} = \text{RCU}(k + \Delta, n) \quad (10)$$

$$\epsilon_u^{\text{ub},1} = \text{RCU}(k + \Delta, n) 2^{-\Delta} \quad (11)$$

with

$$\text{RCU}(k, n) = \mathbb{E} \left[\min \left\{ 1, (2^k - 1) \times \mathbb{P} \left[P_{\mathbf{y}|\mathbf{x}}(\mathbf{y}|\bar{\mathbf{x}}) \geq P_{\mathbf{y}|\mathbf{x}}(\mathbf{y}|\mathbf{x}) | \mathbf{x}, \mathbf{y} \right] \right\} \right] \quad (12)$$

and

$$P_{\mathbf{x}, \mathbf{y}, \bar{\mathbf{x}}}(\mathbf{x}, \mathbf{y}, \bar{\mathbf{x}}) = P_x(\mathbf{x}) P_{\mathbf{y}|\mathbf{x}}(\mathbf{y}|\mathbf{x}) P_x(\bar{\mathbf{x}}). \quad (13)$$

Proof: See Appendix A. ■

Remark 1. *Note that, as we increase Δ , the upper bound $\epsilon_u^{\text{ub},1}$ on the undetected error probability ϵ_u decreases. At the same time, though, the coding rate $R = (k + \Delta)/n$ of the inner code increases, which causes $\epsilon_\tau^{\text{ub},1}$ to increase as well. Also, for $\Delta = 0$, we have $\epsilon_\tau^{\text{ub},1} = \epsilon_u^{\text{ub},1}$, and the right-hand side of both (10) and (11) reduce to $\text{RCU}(k, n)$. Thus, we recover the RCU bound [28, Thm. 16].*

C. Achievability Bound via Generalized Information Density Thresholding

We next state an achievability bound, which, inspired by [30], [31], is obtained by thresholding the so-called generalized information density [37]. Specifically, the decoder seeks the codeword with the highest likelihood and puts out the corresponding message if the generalized information density of this codeword (defined in (16)) is higher than a preset threshold $n\lambda$. Otherwise, the decoder declares an erasure.

Theorem 2. *For an arbitrary input distribution P_x , for all $s > 0$, and for all $\lambda \in \mathbb{R}$, there exists an $(n, k, \epsilon_\tau, \epsilon_u)$ -code for the channel $P_{\mathbf{y}|\mathbf{x}}(\mathbf{y}|\mathbf{x})$ satisfying $\epsilon_\tau \leq \epsilon_\tau^{\text{ub},2}$ and $\epsilon_u \leq \epsilon_u^{\text{ub},2}$, where*

$$\epsilon_\tau^{\text{ub},2} = \widetilde{\text{RCU}}_\lambda(k, n) + \mathbb{P}[\iota_s(\mathbf{x}, \mathbf{y}) < n\lambda] \quad (14)$$

$$\epsilon_u^{\text{ub},2} = \mathbb{E} \left[\min \left\{ 1, (2^k - 1) \tilde{\psi}_{\mathbf{y}, \mathbf{x}}(\mathbf{y}, \mathbf{x}) \right\} \right]. \quad (15)$$

Here,

$$\iota_s(\mathbf{x}, \mathbf{y}) = \log_2 \frac{P_{\mathbf{y}|\mathbf{x}}(\mathbf{y}|\mathbf{x})^s}{\mathbb{E}_{\bar{\mathbf{x}}} [P_{\mathbf{y}|\bar{\mathbf{x}}}(\mathbf{y}|\bar{\mathbf{x}})^s]} \quad (16)$$

is the so-called generalized information density,

$$\widetilde{\text{RCU}}_\lambda(k, n) = \mathbb{E} \left[\min \left\{ 1, (2^k - 1) \times \mathbb{P} \left[P_{\mathbf{y}|\mathbf{x}}(\mathbf{y}|\bar{\mathbf{x}}) \geq P_{\mathbf{y}|\mathbf{x}}(\mathbf{y}|\mathbf{x}) | \mathbf{x}, \mathbf{y} \right] \mathbb{1}(\iota_s(\mathbf{x}, \mathbf{y}) \geq n\lambda) \right\} \right] \quad (17)$$

$$\tilde{\psi}_{\mathbf{y}, \mathbf{x}}(\mathbf{y}, \mathbf{x}) = \mathbb{P} \left[P_{\mathbf{y}|\mathbf{x}}(\mathbf{y}|\bar{\mathbf{x}}) \geq \max \left\{ P_{\mathbf{y}|\mathbf{x}}(\mathbf{y}|\mathbf{x}), \tilde{\lambda}_{\mathbf{y}} \right\} | \mathbf{x}, \mathbf{y} \right] \quad (18)$$

$$\tilde{\lambda}_{\mathbf{y}} = (2^{n\lambda} \mathbb{E}_{\bar{\mathbf{x}}} [P_{\mathbf{y}|\bar{\mathbf{x}}}(\mathbf{y}|\bar{\mathbf{x}})^s])^{1/s} \quad (19)$$

and \mathbf{x} , $\bar{\mathbf{x}}$ and \mathbf{y} are jointly distributed as in (13).

Proof: See Appendix B. ■

Remark 2. *In Theorem 2, $s > 0$ is a parameter of the bound that can be optimized, similar to the input distribution P_x .*

⁷Randomization via time-sharing is not needed to achieve (5) and (6).

Remark 3. The optimal Forney's test (3) can equivalently be expressed as [9, Eq. (15)]

$$P_{\mathbf{x}|\mathbf{y}}(\mathbf{x}|\mathbf{y}) > \frac{2^{nT}}{1 + 2^{nT}}. \quad (20)$$

Using Bayes theorem and taking the logarithm of both sides, we may reformulate (20) as

$$\log_2 \frac{P_{\mathbf{y}|\mathbf{x}}(\mathbf{y}|\mathbf{x})}{P_{\mathbf{y}}(\mathbf{y})} > \log_2 \left(2^k \frac{2^{nT}}{1 + 2^{nT}} \right). \quad (21)$$

Note that if we set $s = 1$ in (16), we can see that the decoding rule employed in Theorem 2 resembles Forney's rule. The key difference is that $P_{\mathbf{y}}(\mathbf{y})$ in (21) is the output distribution induced by the chosen code, whereas $\mathbb{E}_{\bar{\mathbf{x}}} [P_{\mathbf{y}|\bar{\mathbf{x}}}(\mathbf{y}|\bar{\mathbf{x}})]$, which is the denominator of the fraction in (16) for the case $s = 1$, is the output distribution induced by the input distribution $P_{\bar{\mathbf{x}}}$.

Remark 4. If we let $\lambda \rightarrow -\infty$ in (14) and (19), we recover the RCU bound [28, Thm. 16] since $\lim_{\lambda \rightarrow -\infty} \text{RCU}_{\lambda}(k, n) = \text{RCU}(k, n)$, and both $\epsilon_{\tau}^{\text{ub},2}$ and $\epsilon_{\nu}^{\text{ub},2}$ in (14) and (15), respectively, reduce to $\text{RCU}(k, n)$.

D. Saddlepoint Approximation of Pairwise Error Probability

To numerically evaluate the bounds presented in Theorem 1 and Theorem 2, one needs to evaluate a pairwise error probability (namely (41) in Appendix A and (18)) with very high accuracy. Evaluating it via Monte-Carlo averaging is time-consuming for low error probabilities. We next introduce a saddlepoint approximation to evaluate the tail of the sum of independent but not necessarily identically distributed random variables. Then, inspired by [34], we show that this saddlepoint approximation can be utilized to evaluate (41) and (18) for memoryless channels.

Theorem 3. Fix an $\omega \in \mathbb{R}$ and let z_i , $i \in \{1, \dots, n\}$, be independent but not necessarily identically distributed random variables. Also, let $\gamma_i(\zeta)$ be the cumulant generating function (CGF) of z_i , and let $\gamma_i'(\zeta)$ and $\gamma_i''(\zeta)$ denote the first and second derivatives of $\gamma_i(\zeta)$, respectively. Let also $\gamma^{(n)}(\zeta) = \sum_{i=1}^n \gamma_i(\zeta)$, $(\gamma^{(n)}(\zeta))' = \sum_{i=1}^n \gamma_i'(\zeta)$ and $(\gamma^{(n)}(\zeta))'' = \sum_{i=1}^n \gamma_i''(\zeta)$. Suppose that there exists a $\zeta_0 > 0$ such that

$$\sup_{|\zeta| < \zeta_0} \left| \frac{d^4 \gamma_i(\zeta)}{d\zeta^4} \right| < \infty, \quad \forall i \in \{1, \dots, n\} \quad (22)$$

and also positive constants $m_l \leq m_u$ such that

$$m_l \leq \sum_{i=1}^n \gamma_i''(\zeta) \leq m_u \quad (23)$$

holds for all $n \in \mathbb{N}$ and for all $|\zeta| \leq \zeta_0$. Assume that there exists a $\zeta \in [-\zeta_0, \zeta_0]$ satisfying $\omega = (\gamma^{(n)}(\zeta))'$. If $\zeta > 0$, then

$$\mathbb{P} \left[\sum_{i=1}^n z_i > \omega \right] = e^{\gamma^{(n)}(\zeta) - \zeta (\gamma^{(n)}(\zeta))' + \frac{\zeta^2}{2} (\gamma^{(n)}(\zeta))''} \times Q \left(\zeta \sqrt{(\gamma^{(n)}(\zeta))''} \right) + o \left(\frac{1}{\sqrt{n}} \right). \quad (24)$$

If $\zeta < 0$, then

$$\mathbb{P} \left[\sum_{i=1}^n z_i > \omega \right] = 1 - e^{\gamma^{(n)}(\zeta) - \zeta (\gamma^{(n)}(\zeta))' + \frac{\zeta^2}{2} (\gamma^{(n)}(\zeta))''} \times Q \left(-\zeta \sqrt{(\gamma^{(n)}(\zeta))''} \right) + o \left(\frac{1}{\sqrt{n}} \right). \quad (25)$$

Proof: To prove Theorem 3, we follow the steps in [29, App. I], with one crucial difference. Since the random variables z_i for $i \in \{1, \dots, n\}$ are not necessarily identically distributed, we replace [29, Lem. 8] with [38, Thm. 1, Sec. XVI.6] in one of the steps detailed in [29, App. I]. ■

For memoryless channels, the channel law can be factorized as $P_{\mathbf{y}|\mathbf{x}}(\mathbf{y}|\mathbf{x}) = \prod_{i=1}^n P_{y_i|x_i}(y_i|x_i)$; thus, $\log(P_{\mathbf{y}|\mathbf{x}}(\mathbf{y}|\mathbf{x})) = \sum_{i=1}^n \log(P_{y_i|x_i}(y_i|x_i))$. We then obtain the desired saddlepoint approximation for (41) by setting $z_i = \log(P_{y_i|x_i}(y_i|\bar{x}_i))$ and $\omega = \log(P_{\mathbf{y}|\mathbf{x}}(\mathbf{y}|\mathbf{x}))$ for given \mathbf{x} and \mathbf{y} , and by omitting the $o(\cdot)$ terms in (24) and (25). To obtain a saddlepoint approximation for (18), we set instead $\omega = \log \left(\max \{ P_{\mathbf{y}|\mathbf{x}}(\mathbf{y}|\mathbf{x}), \tilde{\lambda}_{\mathbf{y}} \} \right)$.

The saddlepoint approximation in Theorem 3 requires the evaluation of the CGF $\gamma^{(n)}(\zeta)$ and its derivatives (or, equivalently, the evaluation of $\gamma_i(\zeta)$ and its derivatives for all i). One may use Monte Carlo averaging to evaluate $\gamma^{(n)}(\zeta)$ and then numerically evaluate its derivatives; however, this is computationally expensive. Assuming we have an i.i.d. discrete codebook ensemble in which each symbol of every codeword is drawn independently and uniformly from the finite-cardinality input set \mathcal{X} , we can evaluate $\gamma_i(\zeta)$ and its first and second derivatives in closed form as

$$\gamma_i(\zeta) = \log \left(\frac{1}{|\mathcal{X}|} \sum_{x \in \mathcal{X}} e^{\zeta g_{y_i}(x)} \right) \quad (26)$$

$$\gamma_i'(\zeta) = \frac{\sum_{x \in \mathcal{X}} g_{y_i}(x) e^{\zeta g_{y_i}(x)}}{\sum_{x \in \mathcal{X}} e^{\zeta g_{y_i}(x)}} \quad (27)$$

$$\gamma_i''(\zeta) = \frac{\sum_{x \in \mathcal{X}} g_{y_i}(x)^2 e^{\zeta g_{y_i}(x)}}{\sum_{x \in \mathcal{X}} e^{\zeta g_{y_i}(x)}} - \left(\frac{\sum_{x \in \mathcal{X}} g_{y_i}(x) e^{\zeta g_{y_i}(x)}}{\sum_{x \in \mathcal{X}} e^{\zeta g_{y_i}(x)}} \right)^2 \quad (28)$$

where

$$g_{y_i}(x) = \log(P_{y_i|x}(y_i|x)). \quad (29)$$

IV. ERROR DETECTION FOR CA POLAR CODES

We next discuss the design of error detection and decoding strategies for CA polar codes. We start by considering SCL decoding of polar codes [7] as a reference scheme, and we highlight its basic error detection capability, which enables one to trade in a very limited way a reduction of the UEP with an increase of the TEP. Inspired by Theorems 1 and 2, we then introduce two decoding strategies that provide much more flexibility. Specifically, similar to Theorem 1, the first strategy relies on the use of an outer code for error detection. In CA SCL polar codes, this can be achieved by reserving a subset of the bits of the already existing CRC code for error detection. Similar to Theorem 2, the second strategy relies

on a threshold test. Specifically, we consider Forney's optimal test (3), applied to the list of codewords returned by the SCL decoder. This allows us to approximate the metric in (4).

A. CA Polar Codes: SCL Decoding and Error Detection

The reference scheme is based on the serial concatenation of an inner polar code \mathcal{C}_1 with an outer CRC code \mathcal{C}_0 [7], and it is depicted in Fig. 1. At the encoder side, the binary representation $\mathbf{u} \in \mathbb{F}_2^k$ of an arbitrary message $w \in \{1, \dots, 2^k\}$ is encoded via an (h, k) systematic CRC encoder, which appends $\Delta = h - k$ parity bits to the input message. The output of the CRC encoder is denoted by $\mathbf{v} \in \mathbb{F}_2^h$, and it is provided as input to a polar code encoder. We denote by \mathbf{x} the polar code encoder output, which we assume to be matched to the channel input alphabet \mathcal{X} . That is, denoting by n_c the blocklength in bits of the polar code, we have that $\mathbf{x} \in \mathcal{X}^n$ where $n = n_c / \log_2 |\mathcal{X}|$. The outer-code rate is $R_o = k/h$, the inner-code rate is $R_i = h/n_c$, and the overall code rate, expressed in information bits per channel use, is $R = k/n = R_i R_o \log_2 |\mathcal{X}|$. As in Section II-B, we denote by $\mathcal{C} \subset \mathcal{X}^n$ the overall code defined by this concatenation. We denote the outer CRC encoder and the inner polar code encoder as

$$\phi_o : \mathbb{F}_2^k \mapsto \mathbb{F}_2^h \quad \text{and} \quad \phi_i : \mathbb{F}_2^h \mapsto \mathcal{X}^n \quad (30)$$

respectively, whereas, again in agreement with Section II-B, the overall encoding function is $\phi = \phi_i \circ \phi_o$. Following [7], we assume that SCL decoding of the polar code is performed. This yields a list of codewords $\mathcal{L} \subseteq \mathbb{F}_2^h$. Throughout, we shall denote by L the list size. The list is then expurgated by removing all its elements that do not satisfy the outer code constraints, resulting in the list \mathcal{L}_o . Using the shorthand

$$\phi_i(\mathcal{L}_o) = \{\mathbf{x}' \in \mathcal{X}^n | \mathbf{x}' = \phi_i(\mathbf{v}'), \mathbf{v}' \in \mathcal{L}_o\} \quad (31)$$

we can write the final decision, which follows by applying the ML decision criterion to the list \mathcal{L}_o , as

$$\hat{\mathbf{x}} = \arg \max_{\mathbf{x}' \in \phi_i(\mathcal{L}_o)} P_{\mathbf{y}|\mathbf{x}}(\mathbf{y}|\mathbf{x}'). \quad (32)$$

Specifically, the overall decoder returns the message corresponding to the codeword $\hat{\mathbf{x}}$ if \mathcal{L}_o is non-empty. Otherwise, it declares an erasure.

Remark 5. *This decoding algorithm provides only a very limited error detection capability: an erasure is declared whenever \mathcal{L}_o is empty. For a given CRC code and a given polar code, the only degree of freedom at our disposal to control the trade-off between TEP and UEP is the choice of the SCL decoder list size L . A large L results in a TEP that is close to the one attainable by applying the ML decoding rule to the overall code. However, the larger L , the smaller the probability that \mathcal{L}_o will be empty; hence, the higher the UEP.⁸ Conversely, the smaller L , the higher the probability that \mathcal{L}_o will be empty, and, hence, the smaller the UEP, at the expenses of an increased TEP.*

⁸Observe that in the extreme case $L = 2^h$, the list \mathcal{L}_o is always nonempty and TEP and UEP coincide.

B. SCL Decoding with Split CRC (Algorithm A)

As already mentioned, our first strategy to increase our ability to trade TEP with UEP relies on the use of an outer CRC code for error detection, similar to Theorem 1. Specifically, we decompose the CRC code that is already present in CA polar codes in the concatenation of two binary linear block codes $\mathcal{C}_o^{(1)}$ and $\mathcal{C}_o^{(2)}$. The code $\mathcal{C}_o^{(1)}$ has parameters (h, k') , and code $\mathcal{C}_o^{(2)}$ has parameters (k', k) . Under systematic encoding, the second code appends $\Delta_2 = k' - k$ parity bits to the binary representation \mathbf{u} of the information message. The output of the second code encoder is used as input for the encoder of the first code, which appends additional $\Delta_1 = h - k'$ bits to the second encoder output. The overall number of parity bits is $\Delta = \Delta_1 + \Delta_2$. By suitably choosing $\mathcal{C}_o^{(1)}$ and $\mathcal{C}_o^{(2)}$, we can ensure that the concatenation of the two codes is equivalent to the outer code \mathcal{C}_o , resulting in an unmodified encoding function ϕ_o . The concatenation is illustrated in Figure 2.

At the decoder side, the first outer code $\mathcal{C}_o^{(1)}$ is used to expurgate the list \mathcal{L} produced by the polar SCL decoder. That is, the concatenation of $\mathcal{C}_o^{(1)}$ with the inner polar code \mathcal{C}_1 is treated as an (n, k') CA polar code. We denote by \mathcal{L}_1 the list at the output of the SCL decoder, after the expurgation performed via $\mathcal{C}_o^{(1)}$, i.e. $\mathcal{L}_1 = \mathcal{L} \cap \mathcal{C}_o^{(1)}$. Decoding then proceeds as follows.

Case 1: \mathcal{L}_1 is empty. The decoder returns an erasure.

Case 2: \mathcal{L}_1 is non-empty. The decoder computes

$$\hat{\mathbf{x}} = \arg \max_{\mathbf{x}' \in \phi_i(\mathcal{L}_1)} P_{\mathbf{y}|\mathbf{x}}(\mathbf{y}|\mathbf{x}'). \quad (33)$$

If $\hat{\mathbf{x}}$ satisfies the Δ_2 parity-check constraints imposed by the second outer code $\mathcal{C}_o^{(2)}$, then the decoder outputs the message corresponding to $\hat{\mathbf{x}}$. Otherwise, the decoder rejects the decision and outputs an erasure.

In the following, we will refer to the decision rule described above as Algorithm A. It is important to stress that, in Algorithm A, part of the redundancy introduced by the outer code \mathcal{C}_o is used exclusively for error detection. Specifically, the second outer code $\mathcal{C}_o^{(2)}$ is used as an error detection code, applied to the (n, k') CA polar code formed by the concatenation of $\mathcal{C}_o^{(1)}$ with \mathcal{C}_1 .

Remark 6. *Note that Algorithm A reduces to the reference scheme described in Section IV-A whenever $\Delta_2 = 0$ and, hence, $\Delta_1 = \Delta$. In contrast, for $\Delta_1 = 0$, we have that $\mathcal{L}_1 = \mathcal{L}$, which implies that all CRC code constraints are dedicated to error detection. For a fixed list size L , this results in a much lower UEP than the reference scheme, at the cost of a higher TEP. Intermediate values of Δ_1 can be used to achieve a different tradeoff between the TEP and the UEP.*

C. SCL Decoding with Threshold Test (Algorithm B)

Similar to Theorem 2, our second approach relies on a threshold test. Specifically, we modify the SCL algorithm of the reference scheme described in Section IV-A by introducing an additional error detection mechanism in the form of a

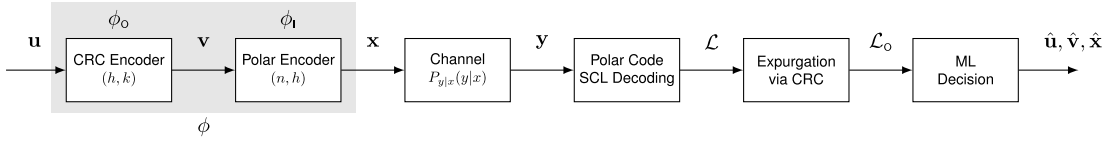


Fig. 1. Reference model describing the encoding with a CA polar code, transmission over the channel, and SCL decoding.

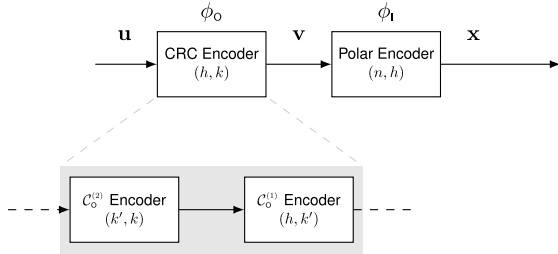


Fig. 2. Decomposition of the outer CRC code \mathcal{C}_o as the concatenation of two binary linear block codes.

threshold test. Namely, upon obtaining the expurgated list \mathcal{L}_o , the decoder operates as follows:

Case 1: \mathcal{L}_o is empty. The decoder returns an erasure.

Case 2: \mathcal{L}_o contains a single element \mathbf{v}' . The decoder outputs the message corresponding to

$$\hat{\mathbf{x}} = \phi_1(\mathbf{v}'). \quad (34)$$

Case 3: \mathcal{L}_o contains more than one element. The decoder computes a preliminary decision according to (32). A threshold test is then performed by computing Forney's test (4) on the codewords in $\phi_1(\mathcal{L}_o)$:

$$\Lambda^{\text{SCL}}(\mathbf{y}, \hat{\mathbf{x}}) = \frac{P_{\mathbf{y}|\mathbf{x}}(\mathbf{y}|\hat{\mathbf{x}})}{\sum_{\mathbf{x}' \in \phi_1(\mathcal{L}_o) \setminus \{\hat{\mathbf{x}}\}} P_{\mathbf{y}|\mathbf{x}}(\mathbf{y}|\mathbf{x}')}. \quad (35)$$

The decision $\hat{\mathbf{x}}$ is accepted if

$$\Lambda^{\text{SCL}}(\mathbf{y}, \hat{\mathbf{x}}) \geq 2^{nT} \quad (36)$$

and it is rejected otherwise, resulting in an erasure.

In the following, we will refer to the decision rule described above as Algorithm B.

Remark 7. Note that in case 1 and case 2 above, the algorithm operates exactly as in the reference scheme reviewed in Section IV-A. The difference resides in case 3, where the reference scheme returns the message corresponding to the codeword in $\phi_1(\mathcal{L}_o)$ that maximizes the likelihood. Instead, Algorithm B relies on a threshold test that approximates Forney's metric (4) by replacing the sum over the codebook with the sum over the expurgated list $\phi_1(\mathcal{L}_o)$. In the limiting case $L = 2^h$, the metric in (35) reduces to Forney's metric (4), which however is not computable for CA polar codes for values of h of practical interest. To summarize, the proposed strategy provides an effective method to implement Forney's rule in CA polar codes.

V. NUMERICAL RESULTS

In this section, we report numerical results to investigate the accuracy of the finite-blocklength bounds proposed in Theorems 1 and 2 in comparison to Forney's bound (5)–(6), as well as the performance of the error detection methods proposed in Section IV for CA polar codes, in relation to the proposed bounds. We also aim to understand when threshold-based schemes should be preferred over solutions based on outer CRC codes. To achieve these goals, we consider two channel models: a biAWGN channel, and a block-memoryless phase-noise channel [33] with pilot-aided phase estimation, quadrature phase-shift keying (QPSK) modulation, and mismatched decoding. We also assume that all codewords \mathbf{x}_m , $m = 1, \dots, 2^k$, in Definition 1 are subject to the power constraint $\|\mathbf{x}_m\|^2 = n$.

The results of CA polar codes are obtained via Monte Carlo simulations. In all simulation results, the polar codes have been designed by selecting the indexes of the h information bits that feature the largest mutual information under genie-aided successive cancellation (SC) decoding [18]. This mutual information is determined via a density evolution (DE) analysis [7], [39], [40] that relies on a Gaussian approximation [41], [42]. To compare the performance of the various decoding algorithms with the achievability bounds presented in Section III, we fix a target total error probability ϵ_T^* and a target undetected error probability ϵ_U^* , and we compute the lowest signal-to-noise ratio (SNR) for which the following two inequalities hold: $\epsilon_T \leq \epsilon_T^*$ and $\epsilon_U \leq \epsilon_U^*$. Specifically, denoting by E_b the energy per information bit, and by N_0 the single-sided AWGN power spectral density, we make use of the following definition:

Definition 2 (SNR threshold). Given a blocklength n , a rate R , and a channel SNR E_b/N_0 , denote by $\mathcal{P}_{n,R}(E_b/N_0)$ the set of achievable pairs (ϵ_T, ϵ_U) . For the target error probabilities ϵ_T^* and ϵ_U^* , the SNR threshold is defined as

$$\gamma(\epsilon_T^*, \epsilon_U^*) = \min \left\{ \frac{E_b}{N_0} \mid (\epsilon_T^*, \epsilon_U^*) \in \mathcal{P}_{n,R}(E_b/N_0) \right\}. \quad (37)$$

For each coding scheme, the reported $\gamma(\epsilon_T^*, \epsilon_U^*)$ is optimized over the parameters of the decoding algorithm. Specifically, for Algorithm A, the optimization involves finding the best split between Δ_1 and Δ_2 , whereas, for Algorithm B, it involves the threshold T in (36).

We also evaluate an upper bound on $\gamma(\epsilon_T^*, \epsilon_U^*)$ by means of the two achievability bounds in Section III, computed by considering an input distribution for which each symbol in each codeword is drawn independently and uniformly from the constellation set. Specifically, given two target TEP and UEP values ϵ_T^* and ϵ_U^* and a given SNR, we set $\Delta = \lceil \log(\epsilon_T^*/\epsilon_U^*) \rceil$ in

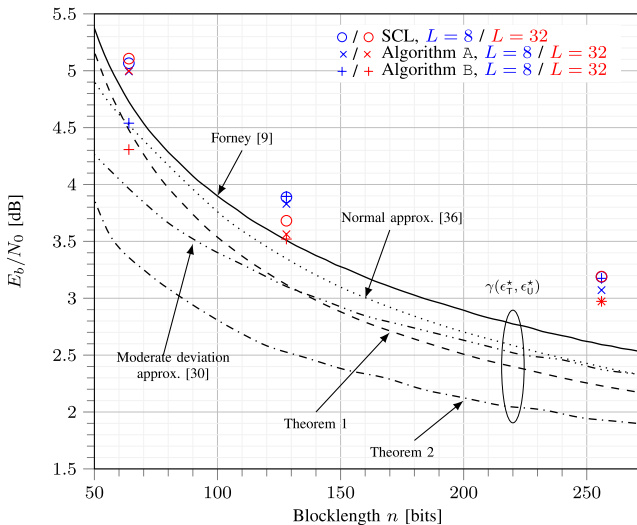


Fig. 3. The minimum E_b/N_0 to achieve $\epsilon_T^* = 10^{-3}$ and $\epsilon_U^* = 10^{-5}$ as a function of blocklength n . Here, we consider a biAWGN channel with $R = 0.5$ bits per channel use.

Theorem 1. Then, we use (10) to evaluate $\epsilon_T^{\text{ub},1}$. If $\epsilon_T^{\text{ub},1} > \epsilon_U^*$ we increase the SNR; otherwise we lower it. This process is repeated until convergence. In the case of Theorem 2, we optimize λ and s so that $\epsilon_U^{\text{ub},2}$ in (15) coincides with ϵ_T^* . Then we evaluate the corresponding $\epsilon_T^{\text{ub},2}$ in (14). If $\epsilon_T^{\text{ub},2} > \epsilon_T^*$, we increase the SNR. Otherwise, we lower it. This process is repeated until convergence. The pairwise error probabilities that appear in the bounds in Theorem 1 and Theorem 2 are computed via the saddlepoint approximation provided in Theorem 3.⁹ In all the results that follow, we set $\epsilon_T^* = 10^{-3}$ and $\epsilon_U^* = 10^{-5}$.

A. Results for the Binary-Input AWGN Channel

We consider binary phase shift keying (BPSK) transmission under the model

$$y_i = x_i + z_i, \quad i = 1, \dots, n. \quad (38)$$

Here, $x_i \in \{+1, -1\}$ and the z_i are independent and identically distributed (i.i.d.), and follow a Gaussian distribution with zero mean and variance σ^2 . For this channel model, we have $E_b/N_0 = 1/(2R\sigma^2)$.

In Fig. 3, we consider the case $R = 1/2$ bits per channel use, and depict the minimum SNR threshold $\gamma(\epsilon_T^*, \epsilon_U^*)$ as a function of the blocklength. Specifically, we illustrate three upper bounds on $\gamma(\epsilon_T^*, \epsilon_U^*)$, obtained via Forney's bound in (5)–(6) and via the two achievability bounds introduced in Theorem 1 and 2, respectively.¹⁰ For completeness, we also report two approximations: the one based on the normal approximation proposed in [36] (which approximates the result

⁹Specifically, for the biAWGN case, we use the numerically efficient implementation of the saddlepoint approximation proposed in [34], whereas the procedure described in Section III-D is used for the block-memoryless phase-noise channel. The code used to plot the bounds can be found at https://github.com/OguzKisilal/ErrorDetection_InfoTheory.

¹⁰The expectations required to evaluate (12), (14), (15), and (17) are evaluated via Monte Carlo simulations.

provided in Theorem 1) and the one based on a moderate-deviation analysis, which follows from [30, Thm. 1] and relies on a threshold decoded similar to the one used in Theorem 2. Three CA polar codes are also considered: a (64, 32) CA polar code based on a 6-bit CRC code (i.e., $\Delta = 6$) with polynomial 0x43; a (128, 64) CA polar code based on a 7-bit CRC code ($\Delta = 7$) with polynomial 0x89; and a (256, 128) CA polar code based on an 8-bit CRC code ($\Delta = 8$) with polynomial 0x1D5. SCL decoding with two list sizes ($L = 8$ and $L = 32$) is considered in the simulations.

We note that the achievability bounds introduced in Theorem 1 and 2 provide a much lower estimate of the minimum SNR threshold than Forney's bound. Furthermore, the achievability bound based on generalized information density thresholding (Theorem 2) provides the lowest estimate.¹¹ Note that the two approximations reported in the figure are not particularly accurate and tend to overestimate the SNR threshold. We also observe that, at very short blocklengths, the gap between the achievability bounds in Theorem 1 and Theorem 2 is the largest: for $n = 64$, the gap is 1.1 dB; it reduces to 0.3 dB when $n = 264$. This result suggests that using a threshold to detect errors is preferable to using an outer CRC code when n is small. The intuition is that, in detection schemes based on an outer CRC code, the inner code rate needs to be increased to compensate for the addition of CRC bits. This is, however, detrimental when n is small.

The results obtained with CA polar codes confirm this observation: the threshold approach used in Algorithm B yields a significant gain over the CRC based approach used in Algorithm A when $n = 64$. Specifically, the gain is approximately 0.5 dB for $L = 8$, and it increases to 0.7 dB for $L = 32$. Interestingly, Algorithm A yields only a limited gain (between 0.1 and 0.2 dB) over the basic error detection capability provided by plain SCL decoding of CA polar codes (see Remark 5). Remarkably, Algorithm B allows one to operate below Forney's achievability bound, as well as below the CRC-based achievability bound given in Theorem 1, and to operate less than 1 dB away from the threshold-based achievability bound of Theorem 2. In agreement with the behavior of the underlying bounds, as the blocklength grows, the gap between the different strategies diminishes. When $n = 128$, Algorithm B still yields the best performance for all the considered list sizes, but it is closely matched by the performance of Algorithm A. When $n = 256$, Algorithm A becomes very competitive: with a list size $L = 32$, its performance is the same as that of Algorithm B; with a list size $L = 8$, it even outperforms Algorithm B, although slightly. This behavior may be explained as follows: as the blocklength grows, the rate penalty introduced by the outer CRC diminishes, and CRCs with a larger number of parity bits can be used. This allows for the exploration of a larger set of pairs (Δ_1, Δ_2) , which enables a finer tuning of the error detection capability provided by the algorithm.

In Fig. 4, we study the behavior of the TEP and UEP as a function of E_b/N_0 for $n = 128$ and $R = 0.5$. All curves

¹¹As we will show in Fig. 9, optimizing over the parameters s is crucial to get such low estimate.

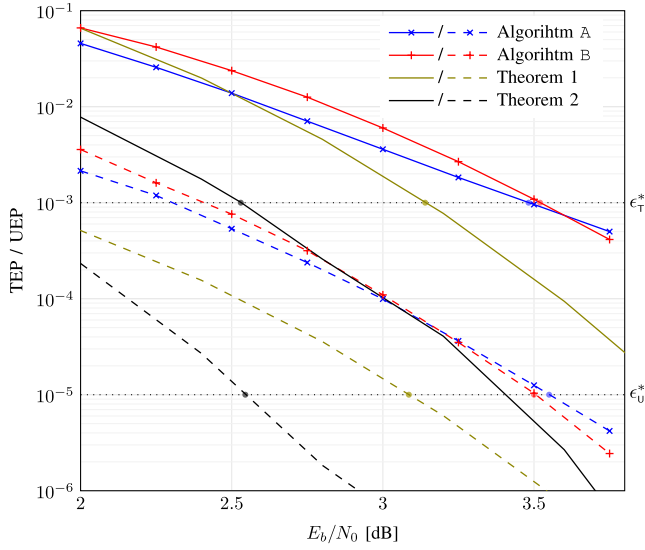


Fig. 4. TEP and UEP versus E_b/N_0 for $(128, 64)$ for CA polar codes under Algorithm A and Algorithm B ($L = 32$). The bounds of Theorem 1 and Theorem 2 are included as a reference. Solid lines are used for the TEP, while dashed lines are used for the UEP. The target TEP and UEP used for the optimization of the error detection parameters are $\epsilon_T^* = 10^{-3}$ and $\epsilon_U^* = 10^{-5}$.

are computed for parameters corresponding to the ones that minimize the SNR threshold for the target $\epsilon_T^* = 10^{-3}$ and $\epsilon_U^* = 10^{-5}$. For the CA polar code, we use SCL decoding with list size $L = 32$. Consistently with the results already presented in Fig. 3, Algorithm A attains the target error probability at $E_b/N_0 \approx 3.55$ dB and Algorithm B attains it at $E_b/N_0 \approx 3.52$ dB. We also report the bounds given in Theorem 1 and Theorem 2 as a reference. Similarly to the result in Fig. 3, the achievability bound obtained through Theorem 2 shows that, for the biAWGN channel, performance can be significantly improved using a decoding strategy based on thresholding the generalized information density.

In Fig. 5, the performance achievable by using the CA polar codes of the 5G NR standard [43] is reported for the case of $R = 0.5$. The 5G NR standard offers a variety of CRC code polynomials, ranging from a 6-bit CRC code to a 24-bit CRC code. In the analysis, the 6-bit CRC code has been used for the blocklength $n = 64$, and the 11-bit CRC has been used for the blocklengths $n = 128$ and $n = 256$. This selection allows minimizing the SNR thresholds achieved by the 5G NR codes for the target error probabilities. In the simulations, the list size has been restricted to $L = 8$. The performance achieved by the 5G NR codes is comparable to the one for the codes provided in Fig. 3. It is possible to observe that, for the two largest blocklengths, the use of a 11-bit CRC provides an error detection capability that exceeds the one required by our optimization target ($\epsilon_T^* = 10^{-3}$ and $\epsilon_U^* = 10^{-5}$), even under standard SCL decoding. Hence, neither Algorithm A nor Algorithm B can provide a gain in this setting. The result may change by setting lower undetected error probability targets.

In Fig. 6, we consider the case $R \simeq 1/3$. Again, CA polar codes designed for three blocklengths ($n = 64, 128, \text{ and } 256$) are considered for the simulations. The CRC codes

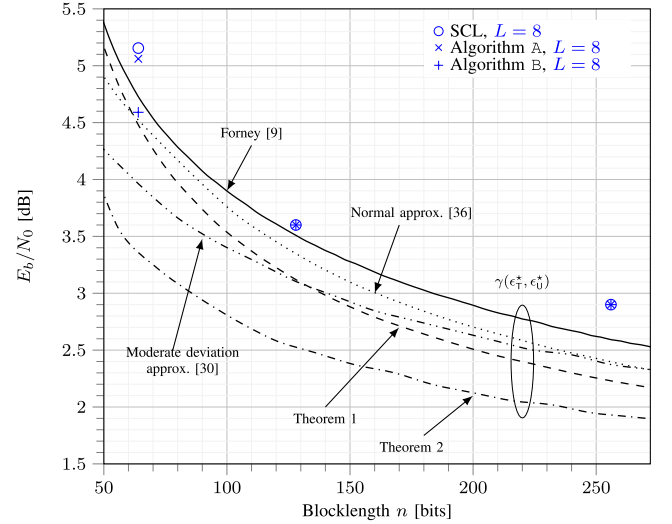


Fig. 5. The minimum E_b/N_0 to achieve $\epsilon_T^* = 10^{-3}$ and $\epsilon_U^* = 10^{-5}$ as a function of blocklength n . The CRC polynomials and the frozen bit set are chosen according to [43]. A CRC-6 is used for $n = 64$, while a CRC-11 is used for $n = 128, 256$. Here, we consider a biAWGN channel with $R = 0.5$ bits per channel use.

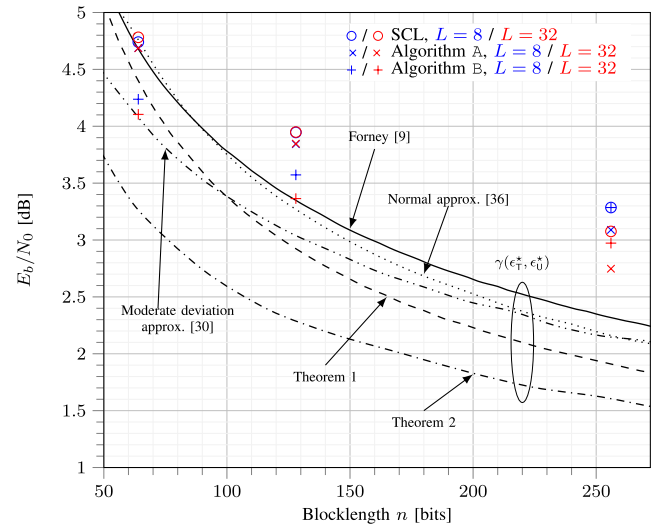


Fig. 6. The minimum E_b/N_0 to achieve $\epsilon_T^* = 10^{-3}$ and $\epsilon_U^* = 10^{-5}$ as a function of blocklength n . Here, we consider a biAWGN channel with $R \simeq 0.33$ bits per channel use.

used in the three cases are the same as the ones used for the rate-1/2 setting of Fig. 3. We see from the figure that most of the insights discussed for the rate-1/2 case extend to the rate-1/3 case, with one notable difference. When $R \simeq 1/3$, Algorithm B clearly outperforms Algorithm A when $n = 64$ and $n = 128$, whereas Algorithm A is clearly preferable when $n = 256$.

In Fig. 7, we consider the case $R = 0.5$ but much lower target TEP and UEP. Specifically, we set $\epsilon_T^* = 10^{-6}$ and $\epsilon_U^* = 10^{-9}$. For this setting, we present only our achievability bounds since the simulation of polar codes at these low error values is challenging. As shown in the figure, for these parameters, Forney's bound provides an estimate of the minimum SNR that is similar to the one provided by

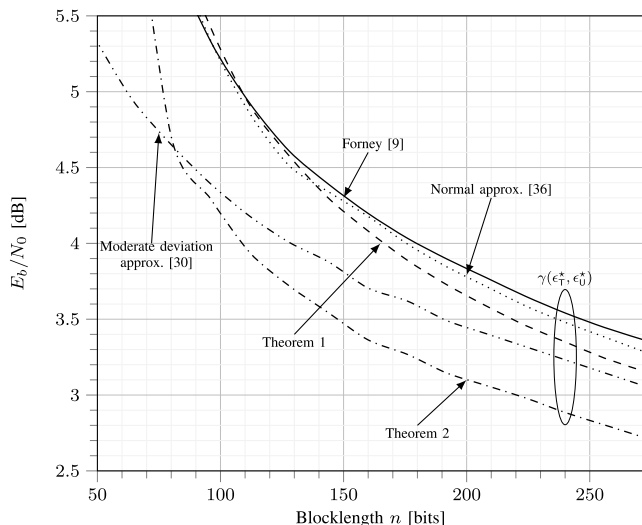


Fig. 7. The minimum E_b/N_0 to achieve $\epsilon_T^* = 10^{-6}$ and $\epsilon_U^* = 10^{-9}$ as a function of blocklength n . Here, we consider a biAWGN channel with $R = 0.5$ bits per channel use.

Theorem 1. However, the estimate provided by Theorem 2 is still much more accurate.

B. Results for the Block-Memoryless Phase-Noise Channel

It is worth highlighting that Forney's optimal threshold test (4), the thresholding scheme used in Theorem 2, and the test (35) performed by Algorithm B all require precise knowledge of the channel law $P_{y|x}$. In contrast, the error detection mechanism used in both the achievability bound in Theorem 1 and by Algorithm A relies solely on a CRC test. It is, therefore, interesting to study how the insights gained via the analysis discussed in Section V-A change in the presence of an imprecise (noisy) knowledge of the channel law, which may originate, for instance, from imperfect CSI. To perform this analysis, we consider the block-memoryless phase-noise channel [33]—a model that is relevant, e.g., for satellite uplink channels with time division multiple access [44]. Specifically, the system relies on QPSK transmission under the model

$$y_i = e^{j\theta} x_i + z_i \quad i = 1, \dots, n. \quad (39)$$

Here, $x_i \in \{\pm\sqrt{2}/2 \pm j\sqrt{2}/2\}$ and the z_i are i.i.d. and follow a complex Gaussian distribution with zero mean and variance $2\sigma^2$. For this channel model, $E_b/N_0 = 1/(2R\sigma^2)$. The phase rotation θ is constant over the packet transmission, and it is drawn independently and uniformly at random from the interval $[0, 2\pi)$ at each packet transmission. We assume that we can estimate the noise variance perfectly (as it does not change from packet to packet). On the contrary, we assume that the receiver has only an estimate $\hat{\theta}$ of the phase rotation θ . Indeed, θ needs to be estimated for each received packet and this may result in a non-negligible estimation error. The receiver proceeds by computing the mismatched likelihoods

$$q(y_i, x_i, \hat{\theta}) = \frac{1}{2\pi\sigma^2} \exp\left(-\frac{1}{2\sigma^2} \left|y_i - e^{-j\hat{\theta}} x_i\right|^2\right) \quad (40)$$

for $i = 1, \dots, n$, which are then provided as input to the decoder. For the analysis, we consider the case where $\hat{\theta}$

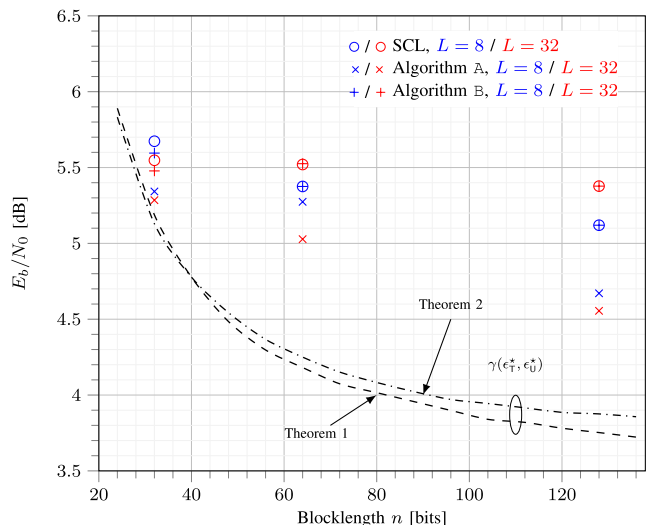


Fig. 8. The minimum E_b/N_0 to achieve $\epsilon_T^* = 10^{-3}$ and $\epsilon_U^* = 10^{-5}$ as a function of blocklength n . Here, we consider QPSK modulated symbols transmitted over a block-memoryless phase-noise channel with 10 pilot symbols and $R = 1$ bits per channel use.

is obtained via ML estimation performed over a pilot field composed by n_p QPSK symbols.¹² Note that the achievability bounds in Theorem 1 and 2 can be evaluated for this setting by replacing $P_{y|x}(y|x)$ with $\prod_{i=1}^n q(y_i, x_i, \hat{\theta})$ and by averaging the bounds over θ and $\hat{\theta}$.

In Fig. 8, we report the minimum SNR required to achieve the target error probability pair $\epsilon_T^* = 10^{-3}$ and $\epsilon_U^* = 10^{-5}$, as a function of blocklength n . The CA polar codes used for the simulations are the same as the one considered in Fig. 3. Since these codes have rate $1/2$ and since we use QPSK modulation, the overall rate is $R = 1$ bits per channel use. To evaluate the robustness to CSI mismatch of the different error detection strategies, we consider a setting where the phase estimate is obtained using only $n_p = 10$ pilot symbols.

We first observe that the gap between the two achievability bounds is largely reduced, with the CRC-based bound in Theorem 1 actually yielding a slightly lower SNR threshold than the threshold-based bound in Theorem 2 as the blocklength increases. The much worse performance of the threshold-based decoding rule of Theorem 2 compared to the biAWGN case analyzed in Fig. 3 can be explained by the high sensitivity to CSI errors of this kind of decoders. Furthermore, while for the biAWGN channel, significant performance improvements can be achieved by optimizing the s parameter in the bound, in the mismatched case such optimization yields only very limited performance gains. To clarify this point, we report in Fig. 9, the minimum SNR required to achieve the target error probability pair $\epsilon_T^* = 10^{-3}$, $\epsilon_U^* = 10^{-5}$ (as predicted by Theorem 2), as a function of the parameter s for both biAWGN and block-memoryless phase-noise channel, with the phase estimated using 10 pilot symbols. We set $k = 50$ for both cases. For comparison, we plot also the minimum

¹²In the results that follow, the energy overhead entailed by the transmission of pilot symbols is neglected: it would only cause a rigid shift of the E_b/N_0 , which applies to all simulation results and achievability bounds.

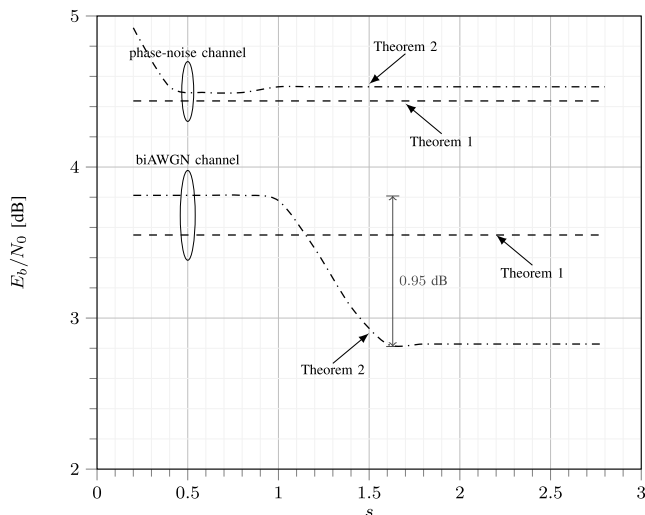


Fig. 9. The minimum E_b/N_0 required to achieve $\epsilon_T^* = 10^{-3}$ and $\epsilon_U^* = 10^{-5}$ as a function of parameter s . Here, we consider $R = 0.5$ bits per channel use for the biAWGN channel, $R = 1$ bits per channel use with 10 pilot symbols for the phase-noise channel; $k = 50$ in both cases.

SNR predicted by Theorem 1, which does not depend on s . We observe that for the biAWGN channel, optimizing over s lowers the minimum required SNR by 0.95 dB. In contrast, for the block-memoryless phase-noise channel, optimizing over s results in a negligible reduction in the minimum required SNR.

Unlike threshold testing, when an outer CRC code is used for error detection, knowledge of the channel law has no impact on the trade-off between ϵ_T and ϵ_U , as this trade-off depends only on the number of CRC bits, as shown in (10)–(11). This observation is confirmed by the simulation results reported in Fig. 8: Algorithm A, which relies on a CRC code for error detection, largely outperforms Algorithm B, which employs the threshold test (35), at all blocklengths. Furthermore, Algorithm B outperforms the reference SCL scheme only when $n = 64$. This result suggests that, in the presence of inaccurate CSI, the use of a CRC-based error detection scheme should be preferred, even at very short blocklengths, over thresholding-based schemes based on mismatched channel likelihoods. Error detection by means of threshold testing is preferable only when sufficiently accurate, albeit imperfect, CSI is available at the decoder.

VI. CONCLUSIONS

We analyzed the trade-off between the total error probability and the undetected error probability in the short blocklength regime by presenting two finite-blocklength achievability bounds, which are used to benchmark the performance of CA polar codes. The first finite-blocklength bound relies on a layered approach, where an outer code is used to perform error detection. The second bound is based on a threshold test applied to the generalized information density. On the biAWGN channel and for blocklengths and error probabilities of interest in URLLC, both bounds are more accurate than Forney’s error-exponent achievability bound, with the bound based on generalized information density providing the best achievability result.

We also presented simulation results for CA polar codes for three error-detection strategies: i) the basic error-detection mechanisms provided by SCL decoding; ii) an algorithm that splits the outer CRC parity bits in two subsets, with one subset dedicated to error detection; iii) a threshold test that approximates Forney’s optimal rule by exploiting the SCL decoder list. Our results for the biAWGN show that, in agreement with the finite-blocklength bounds, the threshold test applied at the output of the SCL decoder yields tangible gains over the outer-CRC-code approach. The gains decrease as the blocklength increases.

However, as illustrated for the case of block-memoryless phase-noise channel, the situation changes drastically when the decoder is fed with imperfect CSI, which results in a mismatched decoding setting. In this case, error detection by means of an outer CRC code exhibits a robust error detection capability, whereas the use of threshold-based techniques that rely on a mismatched likelihood results in a significant performance loss for all blocklength values considered in the paper.

ACKNOWLEDGMENT

The authors would like to thank Prof. Gerhard Kramer (Technical University of Munich) for his constructive suggestions and the anonymous reviewers for their insightful comments that helped improve the final version of this paper.

APPENDIX A PROOF OF THEOREM 1

We consider the case when error detection is provided by an outer $(k + \Delta, k)$ code and error correction by an inner $(n, k + \Delta)$ code. Hence, Δ bits are used for error detection purposes. We can think of the outer code as assigning each message $w \in \{1, \dots, 2^k\}$ to one of 2^Δ bins. The inner encoder maps the k bits describing the message, as well as the Δ bits describing the bin to which the message belongs, to a codeword of a codebook $\hat{\mathcal{C}}$ with $|\hat{\mathcal{C}}| = 2^{k+\Delta}$. Note that, because of the bin assignment, only a subset $\mathcal{C} \subseteq \hat{\mathcal{C}}$ with $|\mathcal{C}| = 2^k$ of codewords is actually used. This procedure allows us to select a subset \mathcal{C} of cardinality 2^k from the codebook $\hat{\mathcal{C}}$ of cardinality $2^{k+\Delta}$. Let us denote by $\mathbf{u} \in \mathbb{F}_2^k$ the binary representation of the message to be transmitted, and by $\mathbf{c} \in \mathbb{F}_2^\Delta$ the binary representation of the corresponding bin index. It will be convenient to write $\mathbf{c} = b(\mathbf{u})$ where the function $b(\cdot)$ returns the binary representation of the index of the bin in which \mathbf{u} is placed.

The decoder first selects a codeword in $\hat{\mathcal{C}}$ uniformly at random among all codewords that have maximum likelihood. If this codeword belongs also to \mathcal{C} , then the corresponding message is returned. If not, the decoder declares an erasure.

Next, we evaluate the average total and undetected error probabilities that are achievable by this coding scheme. Specifically, we average over both the codebook, which is generated by drawing each codeword independently from $P_{\mathbf{x}}$, and the assignment of messages to bins, which we assume is performed uniformly at random.

Let $\hat{\mathcal{C}} = \{\mathbf{x}_1, \dots, \mathbf{x}_{2^{k+\Delta}}\}$. Let also assume, without loss of generality, that the pair (\mathbf{u}, \mathbf{c}) associated to the message to be

transmitted result in the encoder selecting codeword \mathbf{x}_1 . For $m = 2, \dots, 2^{k+\Delta}$, we let

$$\psi_{\mathbf{y},\mathbf{x}}(\mathbf{y}, \mathbf{x}_1) = \mathbb{P}[P_{\mathbf{y}|\mathbf{x}}(\mathbf{y}|\mathbf{x}_m) \geq P_{\mathbf{y}|\mathbf{x}}(\mathbf{y}|\mathbf{x}_1) \mid \mathbf{x}_1, \mathbf{y}]. \quad (41)$$

Note that this quantity is the same for all m since the codewords \mathbf{x}_m are identically distributed. An achievability bound on ϵ_τ follows directly by applying the RCU bound [28, Thm. 16] to the codebook $\hat{\mathcal{C}}$. Specifically,

$$\epsilon_\tau \leq \mathbb{P}\left[\bigcup_{m=2}^{2^{k+\Delta}} P_{\mathbf{y}|\mathbf{x}}(\mathbf{y}|\mathbf{x}_m) \geq P_{\mathbf{y}|\mathbf{x}}(\mathbf{y}|\mathbf{x}_1)\right] \quad (42)$$

$$= \mathbb{E}\left[\mathbb{P}\left[\bigcup_{m=2}^{2^{k+\Delta}} P_{\mathbf{y}|\mathbf{x}}(\mathbf{y}|\mathbf{x}_m) \geq P_{\mathbf{y}|\mathbf{x}}(\mathbf{y}|\mathbf{x}_1) \mid \mathbf{x}_1, \mathbf{y}\right]\right] \quad (43)$$

$$\leq \mathbb{E}\left[\min\left\{1, \sum_{m=2}^{2^{k+\Delta}} \psi_{\mathbf{y},\mathbf{x}}(\mathbf{y}, \mathbf{x}_1)\right\}\right] \quad (44)$$

$$= \text{RCU}(k + \Delta, n). \quad (45)$$

Here, the upper bound in (42) follows by assuming that an error always occurs if more than one codeword has maximum likelihood, (44) follows from the union bound, and (45) follows by letting \mathbf{x} be the transmitted codeword and $\bar{\mathbf{x}}$ be one of the other codewords. To upper-bound ϵ_u , we proceed as follows: let $\hat{m} = \arg \max_{m \in \{1, \dots, 2^{k+\Delta}\}} P_{\mathbf{y}|\mathbf{x}}(\mathbf{y}|\mathbf{x}_m)$ and let the pair $(\hat{\mathbf{u}}, \hat{\mathbf{c}})$ denote the binary representation of the index \hat{m} , where $\hat{\mathbf{u}}$ corresponds to the estimate of the binary representation of the transmitted message, and $\hat{\mathbf{c}}$ is the estimate of the binary representation of its bin index. An error is undetected if $\hat{m} \neq 1$ and $b(\hat{\mathbf{u}}) = \hat{\mathbf{c}}$. Hence,

$$\epsilon_u = \mathbb{P}[\hat{m} \neq 1, b(\hat{\mathbf{u}}) = \hat{\mathbf{c}}] \quad (46)$$

$$= \mathbb{P}[\hat{m} \neq 1] \mathbb{P}[b(\hat{\mathbf{u}}) = \hat{\mathbf{c}} \mid \hat{m} \neq 1] \quad (47)$$

$$\leq \mathbb{P}\left[\bigcup_{m=2}^{2^{k+\Delta}} P_{\mathbf{y}|\mathbf{x}}(\mathbf{y}|\mathbf{x}_m) \geq P_{\mathbf{y}|\mathbf{x}}(\mathbf{y}|\mathbf{x}_1)\right] 2^{-\Delta} \quad (48)$$

$$\leq \text{RCU}(k + \Delta, n) 2^{-\Delta}. \quad (49)$$

Here, (48) follows by using the same bound as in (42); we also used that the probability that the message with binary representation $\hat{\mathbf{u}}$ is assigned to the bin with binary representation $\hat{\mathbf{c}}$ is $2^{-\Delta}$. Finally, (49) follows from the same steps leading to (45). ■

APPENDIX B PROOF OF THEOREM 2

We consider a decoder that outputs the message that corresponds to the codeword that is selected uniformly at random among the codewords with the largest likelihood $P_{\mathbf{y}|\mathbf{x}}(\mathbf{y}|\mathbf{x})$, provided that its generalized information density, defined in (16), exceeds the threshold $n\lambda$; if not, the decoder declares an erasure. We next use a random coding argument and evaluate the average TEP, averaged over random codebooks constructed by drawing each codeword independently from

$P_{\mathbf{x}}$. Let us assume, without loss of generality, that \mathbf{x}_1 is the transmitted codeword. Then,

$$\epsilon_\tau \leq \mathbb{P}\left[\left\{\iota_s(\mathbf{x}_1, \mathbf{y}) < n\lambda\right\} \cup \left\{\iota_s(\mathbf{x}_1, \mathbf{y}) \geq n\lambda, \bigcup_{m=2}^{2^k} P_{\mathbf{y}|\mathbf{x}}(\mathbf{y}|\mathbf{x}_m) \geq P_{\mathbf{y}|\mathbf{x}}(\mathbf{y}|\mathbf{x}_1)\right\}\right] \quad (50)$$

$$\leq \mathbb{P}\left[\iota_s(\mathbf{x}_1, \mathbf{y}) \geq n\lambda, \bigcup_{m=2}^{2^k} P_{\mathbf{y}|\mathbf{x}}(\mathbf{y}|\mathbf{x}_m) \geq P_{\mathbf{y}|\mathbf{x}}(\mathbf{y}|\mathbf{x}_1)\right] + \mathbb{P}[\iota_s(\mathbf{x}_1, \mathbf{y}) < n\lambda] \quad (51)$$

$$= \mathbb{E}\left[\mathbb{P}\left[\bigcup_{m=2}^{2^k} P_{\mathbf{y}|\mathbf{x}}(\mathbf{y}|\mathbf{x}_m) \geq P_{\mathbf{y}|\mathbf{x}}(\mathbf{y}|\mathbf{x}_1) \mid \mathbf{x}_1, \mathbf{y}\right] \times \mathbb{1}(\iota_s(\mathbf{x}_1, \mathbf{y}) \geq n\lambda)\right] + \mathbb{P}[\iota_s(\mathbf{x}_1, \mathbf{y}) < n\lambda] \quad (52)$$

$$\leq \mathbb{E}\left[\min\left\{1, \sum_{m=2}^{2^k} \psi_{\mathbf{y},\mathbf{x}}(\mathbf{y}, \mathbf{x}_1)\right\} \mathbb{1}(\iota_s(\mathbf{x}_1, \mathbf{y}) \geq n\lambda)\right] + \mathbb{P}[\iota_s(\mathbf{x}_1, \mathbf{y}) < n\lambda] \quad (53)$$

$$\leq \widetilde{\text{RCU}}_\lambda(k, n) + \mathbb{P}[\iota_s(\mathbf{x}, \mathbf{y}) < n\lambda]. \quad (54)$$

Here, (51) and (53) follow from the union bound (note that $\psi_{\mathbf{y},\mathbf{x}}(\mathbf{y}, \mathbf{x}_1)$ was defined in (41)); (54) follows by letting \mathbf{x} be the transmitted codeword and $\bar{\mathbf{x}}$ be one of the other codewords.

Similarly, we can bound ϵ_u as

$$\begin{aligned} \epsilon_u &\leq \mathbb{P}\left[\bigcup_{m=2}^{2^k} P_{\mathbf{y}|\mathbf{x}}(\mathbf{y}|\mathbf{x}_m) \geq \max\{P_{\mathbf{y}|\mathbf{x}}(\mathbf{y}|\mathbf{x}_1), \tilde{\lambda}_{\mathbf{y}}\}\right] \quad (55) \\ &\leq \mathbb{E}\left[\min\left\{1, (2^k - 1)\right.\right. \\ &\quad \left.\left.\times \mathbb{P}\left[P_{\mathbf{y}|\mathbf{x}}(\mathbf{y}|\bar{\mathbf{x}}) \geq \max\{P_{\mathbf{y}|\mathbf{x}}(\mathbf{y}|\mathbf{x}), \tilde{\lambda}_{\mathbf{y}}\} \mid \mathbf{x}, \mathbf{y}\right]\right\}\right]. \quad (56) \end{aligned}$$

Here, (55) follows because the condition $\iota_s(\mathbf{x}_m, \mathbf{y}) \geq n\lambda$ is equivalent to $P_{\mathbf{y}|\mathbf{x}}(\mathbf{y}|\mathbf{x}_m) \geq \tilde{\lambda}_{\mathbf{y}}$; (56) follows from steps similar to the ones leading to (54).

With these steps, we have established achievability bounds on the average UEP and TEP, averaged over the random codebook. However, this does not imply the existence of a single deterministic codebook that achieves both bounds simultaneously. To solve this problem, we proceed as in [45, App. A] (see also [35, Thm. 3]), and conclude that the bounds can be achieved by a randomized coding strategy that involves time sharing between two codebooks. Time-sharing is made possible by the introduction of the random variable u (see Definition 1). ■

REFERENCES

- [1] A. Sauter, B. Matuz, and G. Liva, "Error detection strategies for CRC-concatenated polar codes under successive cancellation list decoding," in *Proc. Conf. Inf. Sci. Sys. (CISS)*, Baltimore, MD, USA, Mar. 2023, pp. 1–6.

- [2] G. Durisi, T. Koch, and P. Popovski, "Toward massive, ultrareliable, and low-latency wireless communication with short packets," *Proc. IEEE*, vol. 104, no. 9, pp. 1711–1726, Sep. 2016.
- [3] G. Durisi, G. Liva, and Y. Polyanskiy, "Short-packet transmission," in *Information Theoretic Perspectives on 5G Systems and Beyond*, I. Maric, S. Shamai, and O. Simeone, Eds. New York, NY, USA: Cambridge Univ. Press, 2021.
- [4] T. De Cola, E. Paolini, G. Liva, and G. Calzolari, "Reliability options for data communications in the future deep-space missions," *Proc. IEEE*, vol. 99, no. 11, pp. 2056–2074, Nov. 2011.
- [5] *Next Generation Uplink*, Green Book, Issue 1, Consultative Committee for Space Data Systems (CCSDS) Report Concerning Space Data System Standards 230.2-G-1, Jul. 2014.
- [6] R. Devassy, G. Durisi, G. C. Ferrante, O. Simeone, and E. Uysal, "Reliable transmission of short packets through queues and noisy channels under latency and peak-age violation guarantees," *IEEE J. Sel. Areas Commun.*, vol. 37, no. 4, pp. 721–734, Apr. 2019.
- [7] I. Tal and A. Vardy, "How to construct polar codes," *IEEE Trans. Inf. Theory*, vol. 59, no. 10, pp. 6562–6582, Oct. 2013.
- [8] R. E. Blahut, *Algebraic codes for data transmission*. New York, NY, USA: Cambridge Univ. Press, 2003.
- [9] G. Forney, Jr., "Exponential error bounds for erasure, list, and decision feedback schemes," *IEEE Trans. Inf. Theory*, vol. 14, no. 2, pp. 206–220, Mar. 1968.
- [10] A. Raghavan and C. Baum, "A reliability output Viterbi algorithm with applications to hybrid ARQ," *IEEE Trans. Inf. Theory*, vol. 44, no. 3, pp. 1214–1216, May 1998.
- [11] E. Hof, I. Sason, and S. Shamai, "On optimal erasure and list decoding schemes of convolutional codes," in *Proc. Symposium on Communication Theory and Applications (ISCTA)*, Jul. 2009, p. 6–10.
- [12] A. R. Williamson, M. J. Marshall, and R. D. Wesel, "Reliability-output decoding of tail-biting convolutional codes," *IEEE Trans. Commun.*, vol. 62, no. 6, pp. 1768–1778, Jun. 2014.
- [13] A. Baldauf, A. Belhouchat, S. Kalantarmoradian, A. Sung-Miller, D. Song, N. Wong, and R. D. Wesel, "Efficient computation of Viterbi decoder reliability with an application to variable-length coding," *IEEE Trans. Commun.*, vol. 70, no. 9, pp. 5711–5723, Jul. 2022.
- [14] S. Dolinar, K. Andrews, F. Pollara, and D. Divsalar, "Bounded angle iterative decoding of LDPC codes," in *Proc. IEEE Int. Conf. Mil. Commun.*, San Diego, CA, USA, Nov. 2008, pp. 1–6.
- [15] —, "The limits of coding with joint constraints on detected and undetected error rates," in *Proc. IEEE Int. Symp. Inf. Theory*, Toronto, ON, Canada, Jul. 2008, pp. 970–974.
- [16] M. Jang, J. Lee, S.-H. Kim, and K. Yang, "Improving the tradeoff between error correction and detection of concatenated polar codes," *IEEE Trans. Commun.*, vol. 69, no. 7, pp. 4254–4266, Jul. 2021.
- [17] N. Stolte, "Rekursive codes mit der Plotkin-konstruktion und ihre decodierung," Ph.D. dissertation, Dept. Elect. Eng. and Inf. Technol., Technische Universität Darmstadt, Darmstadt, Germany, 2002.
- [18] E. Arikan, "Channel polarization: A method for constructing capacity-achieving codes for symmetric binary-input memoryless channels," *IEEE Trans. Inf. Theory*, vol. 55, no. 7, pp. 3051–3073, Jul. 2009.
- [19] I. Tal and A. Vardy, "List decoding of polar codes," *IEEE Trans. Inf. Theory*, vol. 61, no. 5, pp. 2213–2226, May 2015.
- [20] R. Pedarsani, "Polar codes: Construction and performance analysis," Master's thesis, Swiss Federal Institute of Technology (EPFL), Jun. 2011.
- [21] N. Merhav, "Error exponents of erasure/list decoding revisited via moments of distance enumerators," *IEEE Trans. Inf. Theory*, vol. 54, no. 10, pp. 4439–4447, 2008.
- [22] A. Somekh-Baruch and N. Merhav, "Exact random coding exponents for erasure decoding," *IEEE Trans. Inf. Theory*, vol. 57, no. 10, pp. 6444–6454, Oct. 2011.
- [23] A. Barg, "Improved error bounds for the erasure/list scheme: the binary and spherical cases," *IEEE Trans. Inf. Theory*, vol. 50, no. 10, pp. 2503–2514, 2004.
- [24] E. Hof, I. Sason, and S. Shamai, "Performance bounds for erasure, list, and decision feedback schemes with linear block codes," *IEEE Trans. Inf. Theory*, vol. 56, no. 8, pp. 3754–3778, Aug. 2010.
- [25] I. E. Telatar, "Multi-access communications with decision feedback decoding," PhD thesis, Mass. Inst. Technol., Cambridge, MA, May 1992.
- [26] I. E. Telatar and R. G. Gallager, "New exponential upper bounds to error and erasure probabilities," in *Proc. Int. Symp. Inf. Theory*, Trondheim, Norway, Jun. 1994, p. 379.
- [27] P. Moulin, "A Neyman–Pearson approach to universal erasure and list decoding," *IEEE Trans. Inf. Theory*, vol. 55, no. 10, pp. 4462–4478, 2009.
- [28] Y. Polyanskiy, H. V. Poor, and S. Verdú, "Channel coding rate in the finite blocklength regime," *IEEE Trans. Inf. Theory*, vol. 56, no. 5, pp. 2307–2359, May 2010.
- [29] A. Lancho, J. Östman, G. Durisi, T. Koch, and G. Vazquez-Vilar, "Saddlepoint approximations for short-packet wireless communications," *IEEE Trans. Wireless Commun.*, vol. 19, no. 7, pp. 4831–4846, Jul. 2020.
- [30] M. Hayashi and V. Y. F. Tan, "Asymmetric evaluations of erasure and undetected error probabilities," *IEEE Trans. Inf. Theory*, vol. 61, no. 12, pp. 6560–6577, 2015.
- [31] V. Y. F. Tan and P. Moulin, "Second-order capacities of erasure and list decoding," in *Proc. Int. Symp. Inf. Theory*, Honolulu, HI, USA, Jun. 2014, pp. 1887–1891.
- [32] M. C. Coşkun, G. Durisi, T. Jerkovits, G. Liva, W. Ryan, B. Stein, and F. Steiner, "Efficient Error-Correcting Codes in the Short Blocklength Regime," *Elsevier Physical Communication*, vol. 34, pp. 66–79, Jun. 2019.
- [33] M. Peleg and S. Shamai, "On the capacity of the blockwise incoherent MPSK channel," *IEEE Trans. Commun.*, vol. 46, no. 5, pp. 603–609, May 1998.
- [34] J. Font-Segura, G. Vazquez-Vilar, A. Martinez, A. Guillén i Fàbregas, and A. Lancho, "Saddlepoint approximations of lower and upper bounds to the error probability in channel coding," in *Proc. Conf. Inf. Sci. Sys. (CISS)*, Princeton, NJ, Mar. 2018.
- [35] Y. Polyanskiy, H. V. Poor, and S. Verdú, "Feedback in the non-asymptotic regime," *IEEE Trans. Inf. Theory*, vol. 57, no. 8, pp. 4903–4925, Jul. 2011.
- [36] P. Wu and N. Jindal, "Coding versus ARQ in fading channels: How reliable should the PHY be?" *IEEE Trans. Commun.*, vol. 59, no. 12, pp. 3363–3374, Nov. 2011.
- [37] A. Martinez and A. Guillén i Fàbregas, "Saddlepoint approximation of random-coding bounds," in *Proc. Inf. Theory Appl. Workshop*, San Diego, CA, USA, Feb. 2011, pp. 257–262.
- [38] W. Feller, *An Introduction to Probability Theory and Its Applications*. New York, NY, USA: Wiley, 1971, vol. 2.
- [39] R. Mori and T. Tanaka, "Performance of polar codes with the construction using density evolution," *IEEE Commun. Lett.*, vol. 13, no. 7, pp. 519–521, Jul. 2009.
- [40] T. Richardson and R. Urbanke, "The capacity of low-density parity-check codes under message-passing decoding," *IEEE Trans. Inf. Theory*, vol. 47, no. 2, pp. 599–618, Feb. 2001.
- [41] S.-Y. Chung, T. J. Richardson, and R. L. Urbanke, "Analysis of sum-product decoding of low-density parity-check codes using a Gaussian approximation," *IEEE Trans. Inf. Theory*, vol. 47, no. 2, pp. 657–670, Feb. 2001.
- [42] P. Trifonov, "Efficient design and decoding of polar codes," *IEEE Trans. Commun.*, vol. 60, no. 11, pp. 3221–3227, Nov. 2012.
- [43] *Technical Specification Group Radio Access Network - NR - Multiplexing and channel coding*, 3rd Generation Partnership Project (3GPP) Technical specification TS 38.212 V16.5.0, Mar. 2021.
- [44] B. Matuz, G. Liva, E. Paolini, M. Chiani, and G. Bauch, "Low-rate non-binary LDPC codes for coherent and blockwise non-coherent AWGN channels," *IEEE Trans. Commun.*, vol. 61, no. 10, pp. 4096–4107, Oct. 2013.
- [45] J. Östman, R. Devassy, G. Durisi, and E. G. Ström, "Short-packet transmission via variable-length codes in the presence of noisy stop feedback," *IEEE Trans. Wireless Commun.*, vol. 20, no. 1, pp. 214–227, Sep. 2021.